Estimates of Site Effectsin the Garhwal Himalaya

GaulkarAmolSudhakar, Ashwani Kumar, S. C. Gupta and Arjun Kumar

Department of Earthquake Engineering, Indian Institute of Technology Roorkee INDIA

Abstract

Three-component digital datafrom a 12-station seismological network in the Garhwal Himalaya have been used estimate the site effectsfrom S-wave componentsof eight local earthquakes and microtremors. These earthquakes ($2.0 \leq M_L \leq 2.92$) have been occurred at epicentral distances between 100 km to 200 km from the center of the network with focal depths ranging from 2.5 km to 22.7 km. S-wave spectral ratios were computed from 273 waveforms in frequency range from 1 to 12 Hz considering PRT as a reference site. H/V spectral ratios in frequency range from 1 Hz to 25 Hz have been estimated from 117 samples of microtremors with duration ranging from 30 seconds to 280 seconds.

From S–wave spectral ratios, higher amplifications have been brought out at sites located nearest to the epicenters of the earthquakes as compared to sites located away from the epicenters. Almost similar frequency dependent trends in the S-wave site amplifications in the radial and transverse components have been brought out at the majority of sites.High amplificationaround 10 Hz at CHN site seems to be due to topographic effect as the site is located on 2244 m high mountain peak. At most of the sites, the vertical components show consistently low site amplifications as compared to horizontal components particularly at frequencies above 4 Hz to 5 Hz. H/V spectral ratios from the microtremorsof morning hours have showndominant broad peaks between 3 Hz and 4 Hz at CNT, PRT, NTT and RAJ sites, whereas at all sites microtremors recorded in the afternoon show maximum peaks between 2 Hz and 4 Hz, and beyond 4 Hz the amplifications decreases. An interesting feature at NTT and AYR sites, is a sharp peak embedded in a broad peak around 4 Hz. This response seems to be due to the vibrations generated by the operation of turbines which are within the radius of 2 km to 3 km from the sites.

Keywords: S-wave, HVSR method, microtremor, amplification, Garhwal Himalaya.

Introduction

The estimation of amplification of ground motion from seismological data has been the subject of many studies using different approaches (e.g. Borcherdt, 1970; Phillips and Aki, 1986; Su et al., 1996; Bonilla et al., 1997). It has been observed that ground motion in the frequency range from 1 to 12 Hz is of most engineering interest and is strongly affected by local site conditions such as local topography and complex surface geology (Su and Aki, 1995). For microzonation of a given region, the site response characteristics form one of the most important inputs. Site response studies are used to quantify the amplification of ground motion and to determine natural resonance frequencies. Therefore, the frequency dependent amplification forms an important component of the seismic hazard analysis. Aim of most of the site response studies hasbeen to identify regions having high seismic hazard due to amplification of ground motion due to the surface geology. This might lead to resonance in case natural frequency of the soil coincides with the natural frequency of the structure. In present study an attempt has been made to estimate the site amplification at eleven sites located in the Garhwal Lesser Himalayawhich is a seismically active region and located between the two major boundary thrust (i.e., the MBT and the MCT). The purposeof study is toquantify the site response in the frequency range from 1 Hz to 12Hz using S-wave spectral ratio method. In addition microtremors data has been used to estimate H/V spectral ratio in the frequency range from 1 Hz to 25 Hz.

Data Used

A 12-station radio-linked local seismological network has been deployed in theGarhwal Lesser Himalaya for the purpose of monitoring the local seismicity in the environs of Tehri dam. The three-component digital data of eight local earthquakes recorded on 12-stations of this network have been used in the present study. The locations of the epicenters of the earthquakes are shown in the Fig 1. The digital data has been collected employing a triaxial short-period seismometer (CMG 40T-1, frequency range: 1 Hz – 100 Hz) coupled to a 24-bit data acquisition system (DAS 130-01/03). At each site, the data is sampled at the rate of 100 samples /second /component. All the local events considered in the analysis have occurred at the epicentral distance range between 100 km and 200 km from the centre of the network. The hypocetnter parameters and local magnitudes of the events are listed inTable 2.

Methodology

Site response can be estimated adopting theoreticalas well as empirical approaches. The theoretical approach allows computing the response by taking a large number of possible input ground motions. However, it requires the detailed knowledge of geotechnical parameters. The empirical approach makes use of either a reference site or a non-reference site. Reference site technique is based on the premise that the two sites have similar source and path effects and the reference site has the flat spectrum response as compared to the site of interest. The site response is estimated by dividing the spectrum of the site of interestby that of a nearby reference site situated on a hard rock. This is also called the spectral ratio method and was introduced by Borcherdt (1970) and has been widely used in different regions of the world (e.g., Margheriti et al., 1994).

The site response is also computed by dividing the spectrum of the horizontal component by that of vertical component recorded at the same site. On similar lines a techniqueto analyze microtremors was introduced by Nakamura (1989).

(a) S-wave spectral ratio method

In this method the site response is computed by taking the spectral ratios of S-waves at the site of interest to the reference site. By taking ratios the source and path effects are eliminated when the distance between the reference site and site of interest is small as compared to the source-to-site distance. A seismogram is represented as the convolution of the source, path, site and instrument response in the time domain and its frequency domain representation is given as (Bonilla et al., 1997):

$$A_{ij}(f)=S_i(f)P_{ij}(f)G_j(f)I_j(f) \qquad \textbf{(1)}$$

where, 'i' is the event and 'j' is the station. S_i (f) - source term of the i_{th} event,$P_{ij}(f)$-path term between the i_{th}event and the j_{th} station,$G_j(f)$-the site term for the j_{th} station, and $I_j(f)$-Instrument response term for the j_{th} station.

After removing the instrument response at each site, the spectral ratios are (Bonilla et al., 1997):

$$A_{ij}(f)\ /A_{ik}(f)=S_i(f)P_{ij}(f)G_j(f)\ /\ S_i(f)P_{ik}(f)G_k(f) \qquad \textbf{(2)}$$

The effect of source term may not be same for the j_{th} and k_{th} sites because of focal mechanism and directivity effects, however, by using a large number of such event-station pairs in small areas these effects are likely to be averaged out. Thus, the equation 2 can be rewritten as:

$$A_{ij}(f)\ /A_{ik}(f)=\ P_{ij}(f)G_j(f)\ /\ P_{ik}(f)G_k(f) \qquad \textbf{(3)}$$

If the distance between the j_{th} and k_{th} sites is less than the hypocentral distances, then it is reasonable to assume that the path term for both the stations are the same (Bonilla et al., 1997). The spectra are corrected for the geometrical spreading by multiplying each spectrum at the j_{th} station for the i_{th}event by its corresponding (S-P) time and assuming that the effect of $Q_{s\ i}$ is negligible. The equation 3 can then be expressed as:

$$A_{ij}(f) / A_{ik}(f) = T_{ij}(f) G_j(f) / T_{ik}(f) G_k(f) \quad \textbf{(4)}$$

Where, $T_{ij}$is the (S-P) time for the i_{th} event at the j_{th} station. Thus, the amplification or the de-amplification is computed at the j_{th} site for the i_{th} event relative to the reference site. The reference site should be located on hard rock and to allow computing spectral ratios, most of the events should be recorded on it.

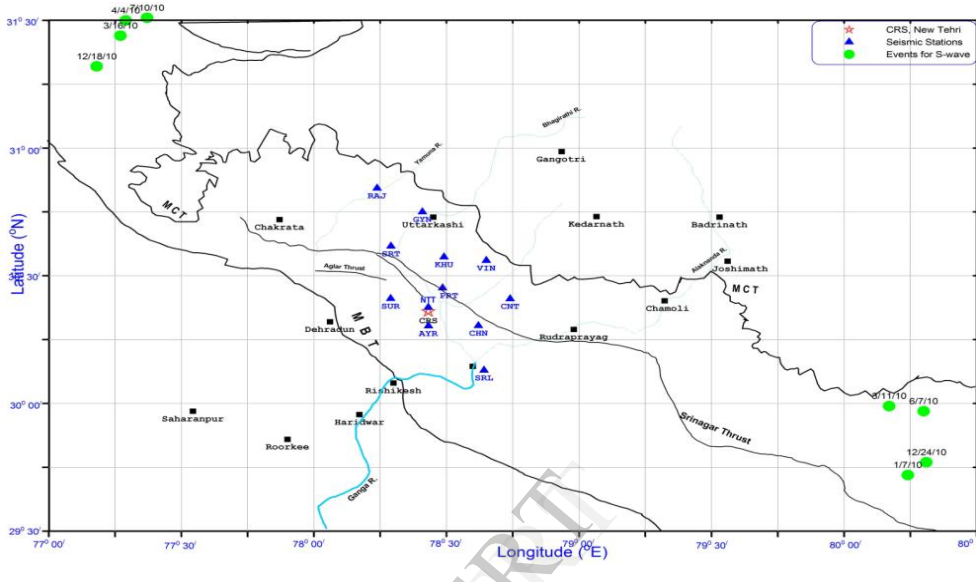

Figure 1 Map showing the location of the events used in the study.

Table 1 Details of recording sites of seismological network.

No.	Station Name	Station Code	Lat.(^{0}N)	Long.(^{0}E)	Rock Type	Elevation (Meters)
1.	Ayarchali	AYR	30-18.18	78-25.86	Sandstone	2106
2.	Chandrabadni	CHN	30-18.31	78-37.14	Phyllites	2244
3.	Chintarbagi	CNT	30-24.59	78-44.69	Phyllites	1953
4.	Khurmola	KHU	30-34.81	78-29.68	Sandstone	1730
5.	New Tehri	NTT	30-22.58	78-25.78	Slates	1914
6.	Pratapnagar	PRT	30-27.48	78-28.54	Quartzite	2128
7.	Sirala	SRL	30-07.92	78-38.03	Sandstone	1424
8.	Srikot	SRT	30-36.76	78-17.93	Phyllites	1617
9.	Surkanda Devi	SUR	30-24.66	78-17.39	Sandstone	2754
10	Giyanja	GYN	30-45.34	78-25.26	Sandstone	2113
11.	Rajgadi	RAJ	30-50.64	78-14.29	Sandstone	1908
12.	Vinakkhal	VIN	30-33.99	78-39.32	Phyllites	1640

Table 2 Hypocenter parameters and magnitudes of the local events used in the S-wave spectral ratio study

No	Date	Origin Time Hr:Mn:Sec	Lat.(°N)	Long.(°E)	Depth Km	Magnitude M_L
1	010710	19:56:32	29.72	80.24	6.83	2.92
2	060710	19:08:23	29.97	80.30	2.50	2.83
3	031110	22:38:18	29.99	80.17	10.76	2.0
4	241210	15:36:30	29.77	80.31	11.01	2.29
5	100710	16:49:22	31.51	77.37	22.72	2.83
6	040410	18:18:21	31.50	77.29	8.43	2.49
7	160310	22:44:45	31.44	77.27	16.77	2.44
8	181210	05:57:54.4	31.32	77.18	9.55	2.47

(b) H/V spectral ratio method

The H/V spectral ratio method also called the "Nakamura technique"(Nakamura, 1989).The technique makes use of H/V spectral ratio of microtremorsto compute the dynamic characteristics of the ground or the structure precisely.The technique assumes is that the vertical component is not affected by the local site geology, whereas the horizontal components get affectedby the local geology underlying the rock site. In view of this, the resonant periods and the site amplification are determined by dividing the horizontal component spectrum by the vertical component spectrum recorded at the same site, thereby eliminating the need for a reference site. This technique is most effective in estimating the natural frequency of soft soil sites when there is a large impedance contrast with the underlying bedrock.

Data analysis by S-wave spectral ratio method.

From the three component record of digital data the analysis of seismograms of S-wave recorded digitally, a time window of a 5.12- sec containing prominent part of the S-wave was selected for the computation of the Fourier spectra(Figure 3 (b)).The two horizontal components are rotated into the radial (R) and transverse (T) components. The radial direction is along the line from the station to the event and the transverse direction is in the horizontal plane at a right angle to the radial direction (Figure 2).

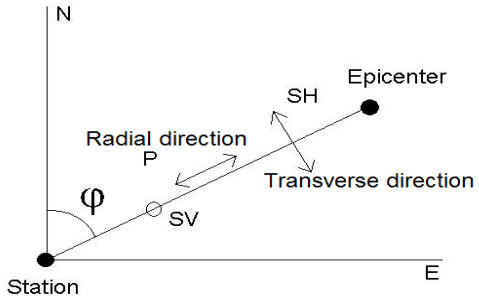

Figure 2 Definition of radial and transverse directions (After Havskov&Ottemoller, 2009).

The rotation is computed using

$$\text{Radial} = -NS\cos(\varphi) - EW\sin(\varphi) \quad (5)$$

$$\text{Transverse} = -NS\sin(\varphi) - EW\cos(\varphi) \quad (6)$$

Where,

φ is the back azimuth angle, defined as the angle between the north and the radial direction (Fig.2).The east-west and north-south components were rotated with respect to their azimuth to the epicenter using the equations 5 &6. The base line and the bit weight corrections were applied to the

data before rotating the horizontal components. Figures 3 (a) and (b) show the three components velocity seismograms of an earthquake recorded at PRT site on July 06, 2010 and its rotated radial and transverse components.

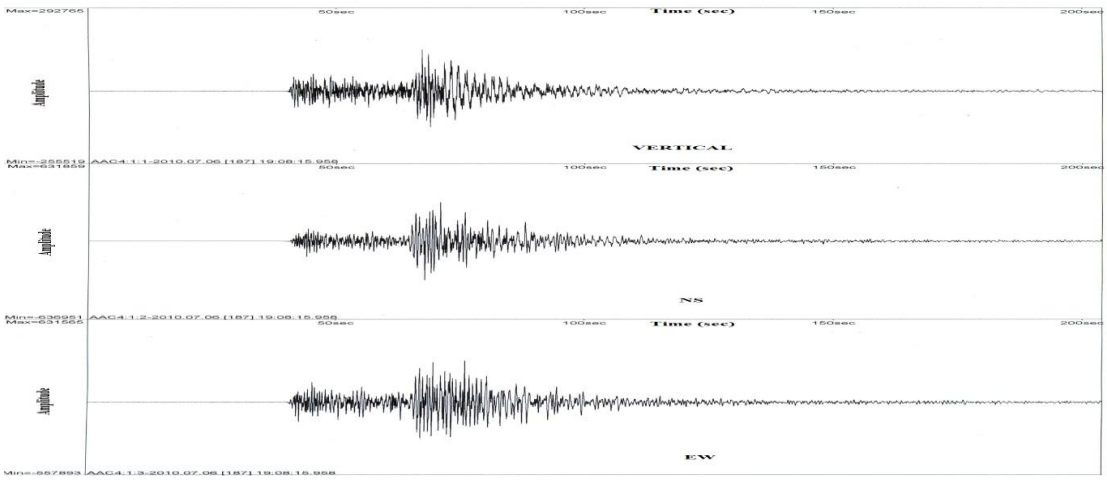

Figure 3 (a) Vertical, NS and EW component seismograms of 06-07-2010 earthquake at PRT station.

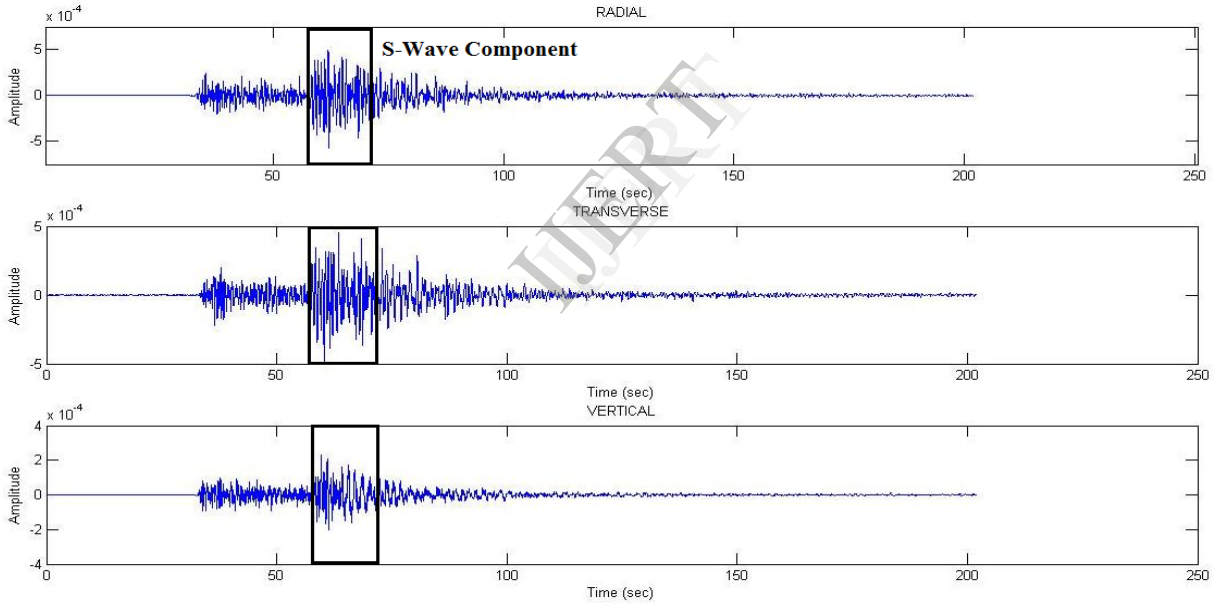

Figure 3 (b) Rotated components of seismogram at PRT station for 06-07-10 earthquake shown with selected S-wave part of waveform used in analysis.

After applying instrument correction and cosine tapering to all the recordings, Fourier amplitudes of S waves are computed using the Fast Fourier Transform (FFT). Each station-event pair was independently analyzed. The onset times of S-wave on the seismograms were visually determined (Figure 3 (b)) and for each event, same time window of the S-wave has been considered for computing the Fourier spectra. The Fourier amplitudes of S-wave were averaged over frequency bands centred at 1.0, 2.0, 3.0, 4.0, 6.0, 8.0, 10.0 and 12.0 Hz respectively in order to get the stable estimates of the amplitudes at these frequencies. The band widths are $\pm$0.5 Hz for 1.0 Hz, $\pm$1.0 Hz for 2.0 and 3.0 Hz bands and for the remaining frequencies it is $\pm$ 2.0 Hz. Thus, the direct spectral ratio of each component at each station has been calculated with respect to the reference station.

Computation of H/V ratios from microtremors

JSESAME software - a dedicated software developed under the European research project SESAME (Site Effects' assessment using Ambient Excitations) has been adopted to compute the H/ V ratio (Atakan*et al.,* 2004). The main steps in the processing are (i) Reading of input time histories in SAF or GSE format, (ii) Offset removal for each selected time window inside time histories for the DC bias removal if any, (iii) Tapering is done to taper the signal from both ends to reduce leaking modes (iv) Conversion to Frequency domain using FFT, (v) Smoothing of Fourier spectra (vi) Merging of horizontal components, (vii) Computing H/V ratio and then the output of single window H/V and (viii) Average of H/V and computation of resonance frequency.Since the software takes only SAF and GCE format, conversion programs available with the SEISAN package were used to convert the recorded time series to SAF format.The software allows both the manual as well as automatic selection of signal windows for processing of data.In the present analysis a 2 sec window length has been selected and the minimum numbers of windows considered in the analysis were ranged from 5 to 20.

Results & Discussion

Siteeffects from S-wave spectral ratio method

Site amplification estimated from the average of four events located at a distance of about 200 km towards southeast from the center of the network and from the average of the four events located at a distance of 170 km towards northwest from the center of the network and average from all the eight events are discussed separately with PRT as reference site.

Fig.4 shows site amplification for radial, transverse and vertical components at 11 sites with reference to PRT site for events occurring to southeast of network. Almost similar frequency dependent trends have been observed at CHN, CNT, and SIR site. Further the pattern of site amplification observed at RAJ site is almost similar to GYN sites and that observed at AYR site is similar to VIN sites. Maximum site amplification of the order of 4 times has been observed at CHN site around 10 Hz. This high amplification seems to be due to the high topography of the site as the site located at a height of 2244 m. Less site amplification has been brought out at RAJ, SRT, KHU sites, whereas GYN, NTT, KHU sites show some peaks at some frequencies. AYR and CNT site shows 2.5 to 3.5 times amplification for transverse component. SIR site shows lesser amplification at lower frequency range up to 4 Hz and thereafter it shows increasing trend in all components with maximum amplification of the order of more than 2 around 10 Hz for transverse component.

Fig.5 shows the site amplification for radial, transverse and vertical components at 11 sites with reference to PRT site for events occurring to the northwest of the network. At nine sites almost similar frequency dependent trend in the site amplification has been brought out for the radial and transverse components. For SUR and KHU sites, this is not true. At KHU site, the site amplification of radial and vertical components has been observed at low frequencies around 3 Hz and 5 Hz respectively, whereas SUR site the site amplification in only transverse component has been brought out around 8 Hz. It is conspicuous to observe that maximum site amplification of the order of 6, 5 and 4 times in the transverse component around frequencies 12 Hz, 8 Hz and 8 Hz has been observed at CHN, RAJ and SUR sites respectively. At low frequencies less than 4 Hz de-amplification has been brought out at NTT, CNT and SIR sites. At all the sites the vertical component shows consistently low site amplifications compared to horizontal components particularly at high frequencies more than 4 Hz to 5 Hz. Comparison of the site response at RAJ and GYN sites has demonstrated that for two horizontal components the trend is almost same, whereas for the vertical component there is a broad peak around 4 Hz at GYN site and a broad peak from 4 Hz to 8 Hz at RAJ site.

Fig 6 shows the site amplification for radial, transverse and vertical components at 11 sites with reference to PRT site by taking the average of eight events. Almost similar frequency dependent trend in the S-wave site amplification in the radial and transverse components has been brought out at

majority of sites. Maximum site amplification of the order of five times has been observed at CHN site around frequency 10 Hz. It is interesting to note that VIN, AYR sites are located closer to PRT site have brought out almost similar trend in the site amplification in all the three components.

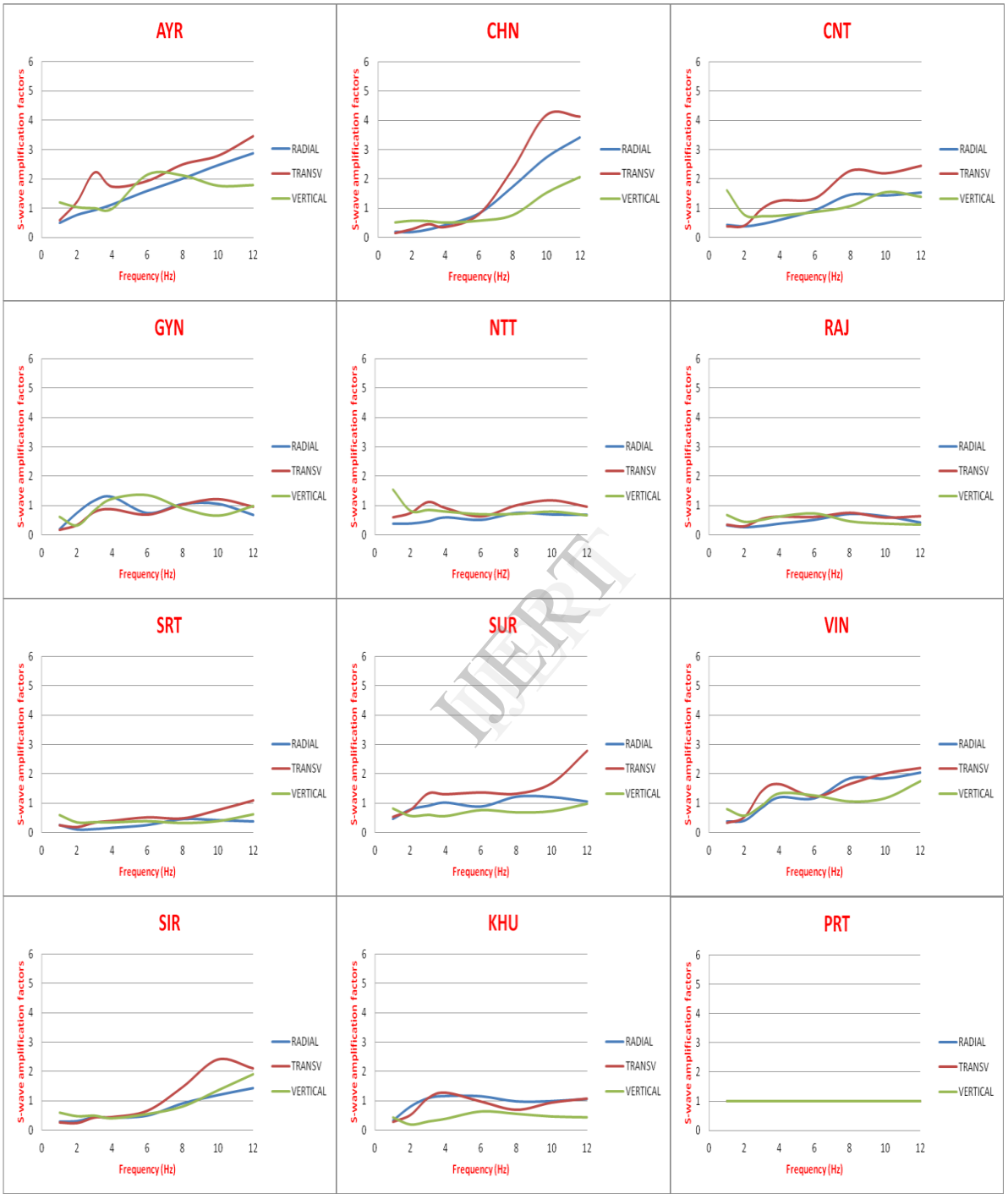

Fig. 4 S-Wave site amplification factor for the average of four earthquakes relative to PRT site at southeast of the

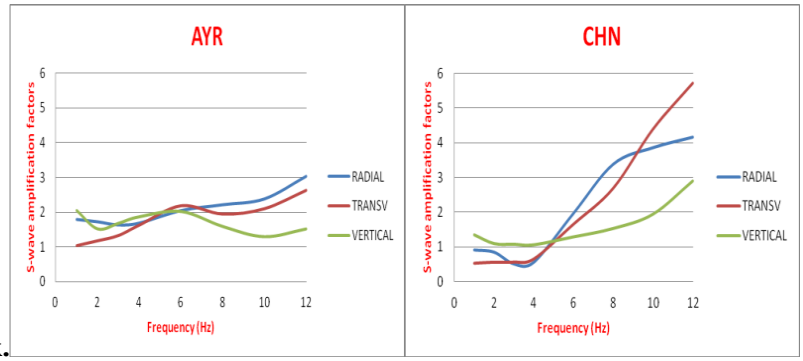

network.

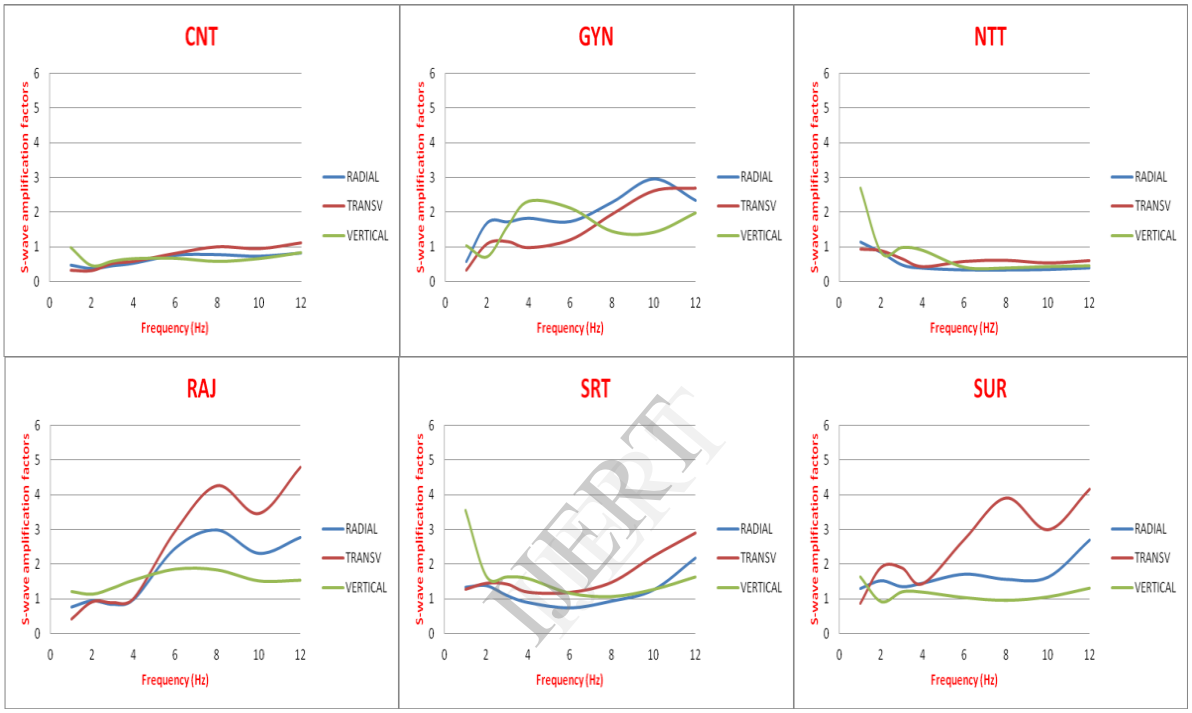

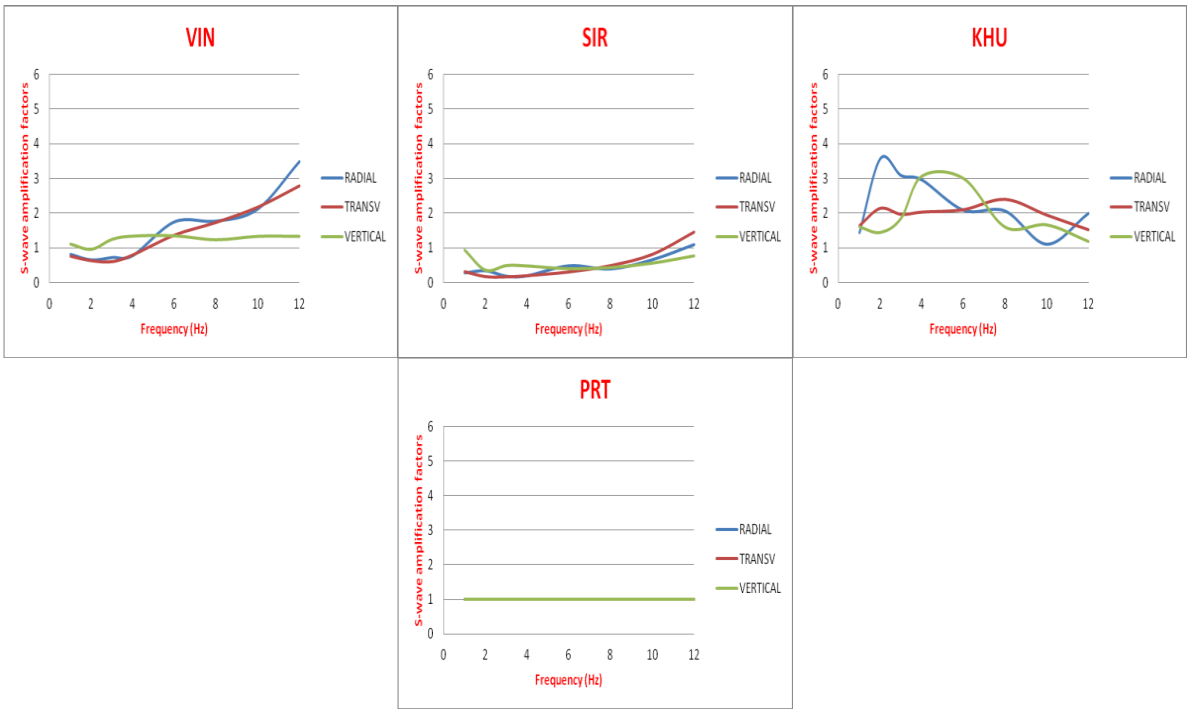

Fig. 5 S-Wave site amplification factor for the average of four earthquakes relative to PRT site at northwest of the network.

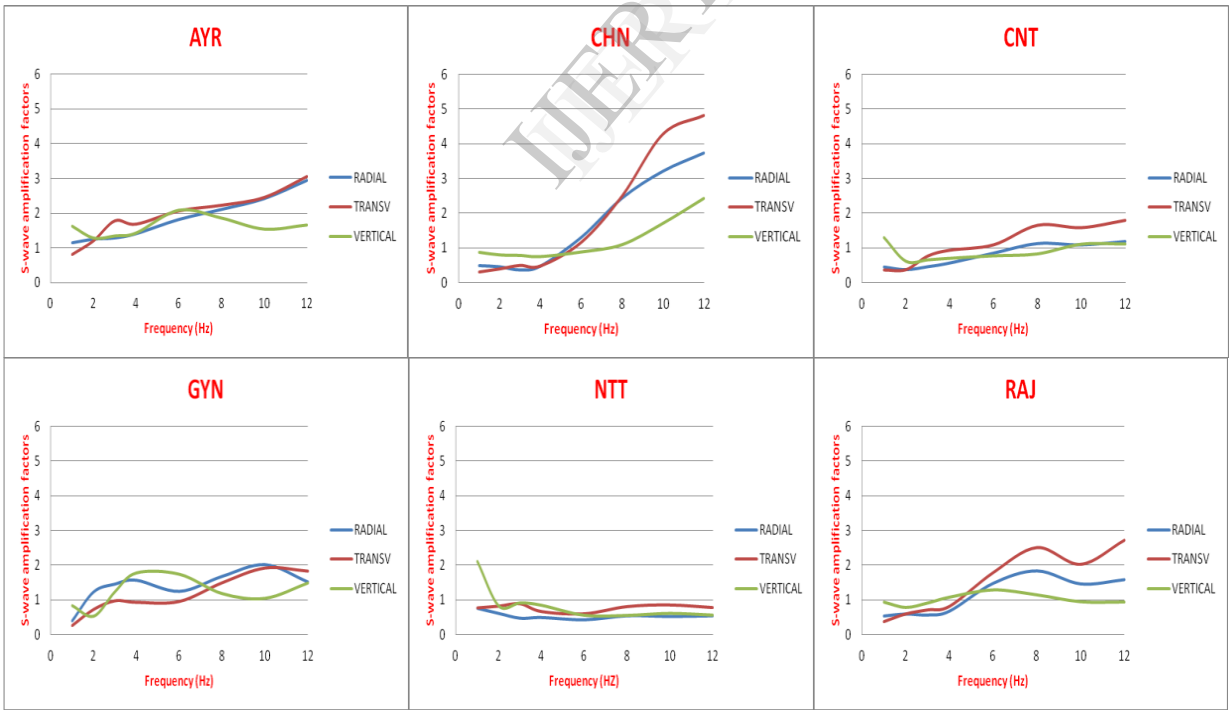

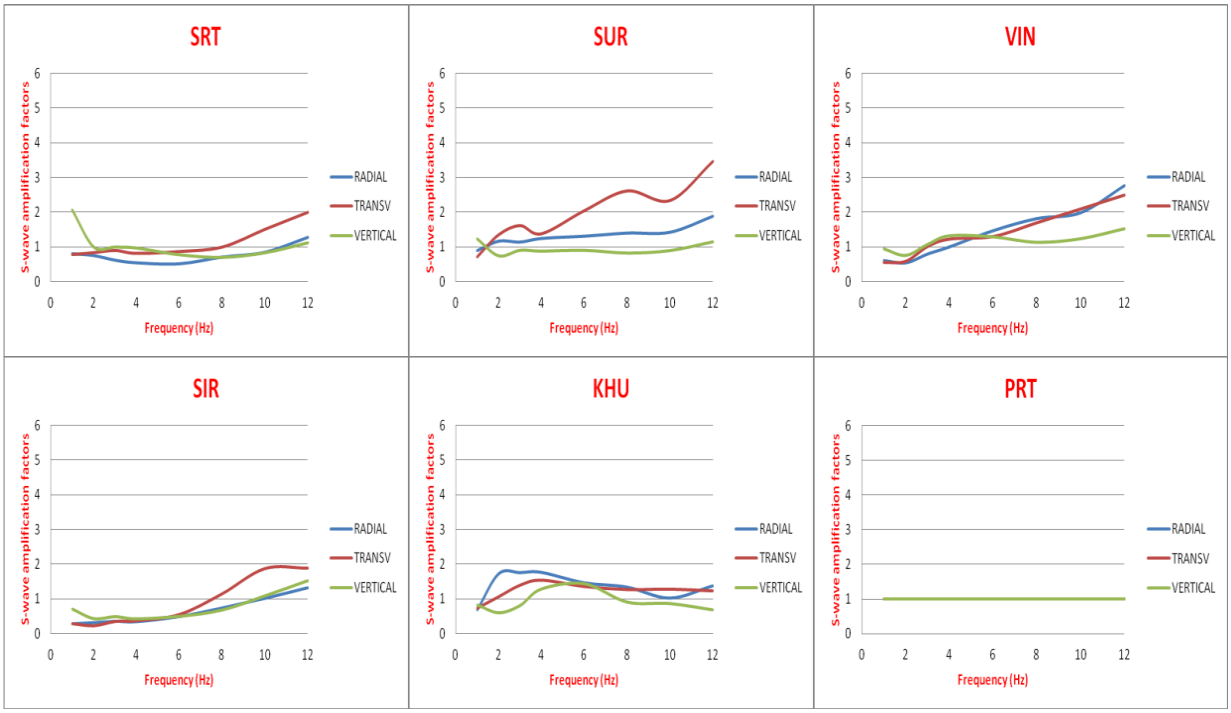

Fig. 6 S-Wave site amplification factor for the average of eight earthquakes relative to PRT site.

Site effects from microtremors using H/V spectral ratio method

The predominant frequency and amplification factor at the predominant frequency as interpreted from the curves are listed in Table 3 for all the four events considered in the analysis.

Figure 7 shows the response of H/V ratio for the micro-tremors data of about 30 seconds recorded by the network on 28 May 2010 around 12:55 p.m.has been analyzed and interpreted.At SUR site, maximum amplification of the order of 6 times in the frequency range from 2 Hz to 4Hz has been observed. The common trend in all the sites is that the amplification values go on decreasing after 4 Hz and have their maximum peak in between 2 Hz to 4 Hz. At RAJ site low amplification have been observed after 8 Hz.

Figure 8 shows the response of H/V ratio for the micro-tremors data of about 45 seconds recorded by the network on 01 May 2010 around 04:06 a.m. has been analyzed and interpreted. Maximum response has been observed at SUR and KHU sites of the order of 4 to 6 times in the frequency range from 1 Hz to 5 Hz. The dominant peaks are between 3Hz to 4 Hz. The site response at NTT and AYR sites is almost identical in the frequency range from 1 Hz to 7 Hz with a sharp peak embedded in a broad peak around 5 Hz. The sharp peak around 5 Hz seems to be due to the continuous vibrations generated by the operation of turbines which are within the radius of 2 km to 3 km from the sites. Further SUR and NTT sites have almost similar peak around 15 Hz. For the case of CHN it has increasing trend after 9 Hz. VIN site have lowest amplification.

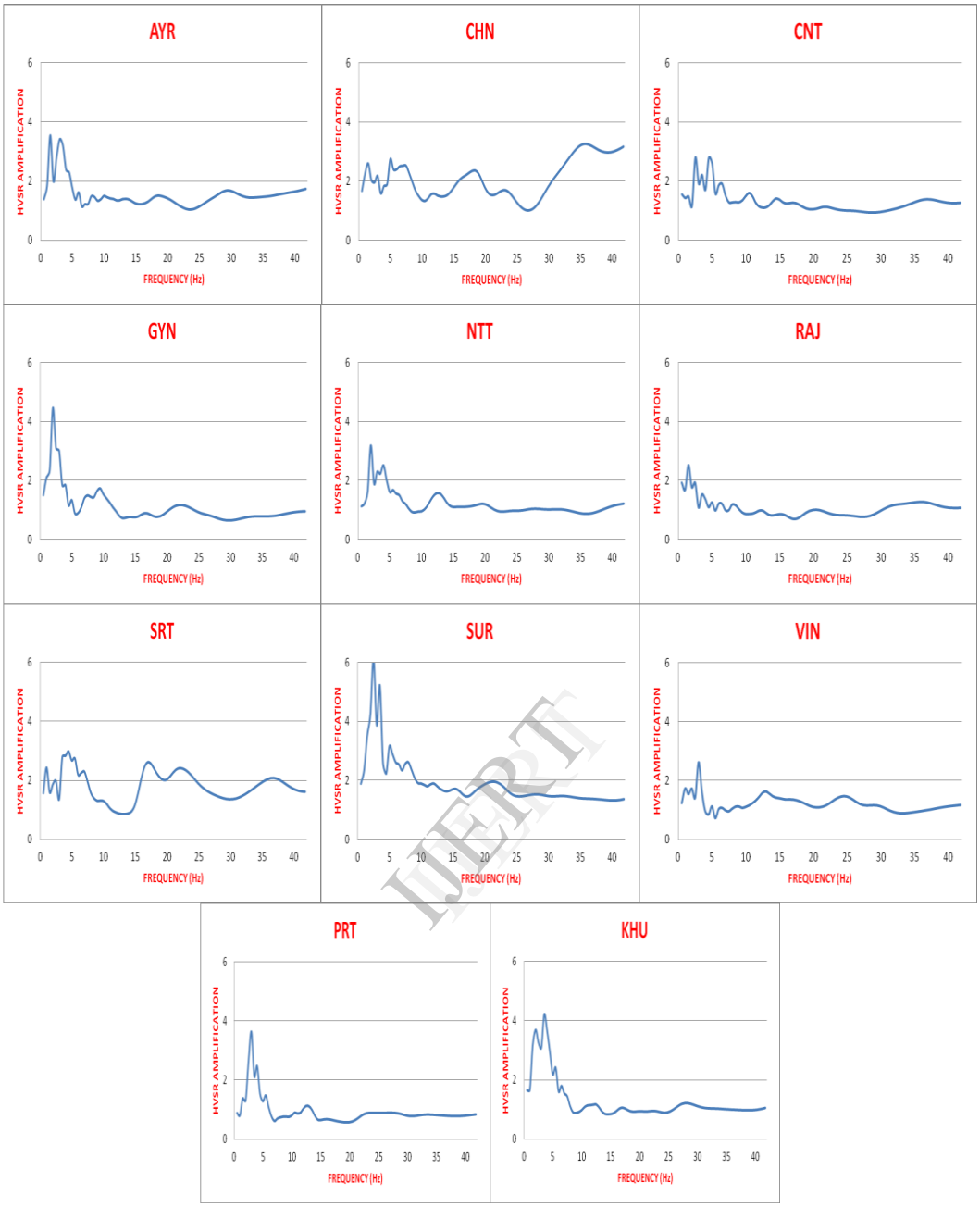
AYR
CHN
CNT
GYN
NTT
RAJ
SRT
SUR
VIN
PRT
KHU
HVSR AMPLIFICATION
FREQUENCY (Hz)
0
2
4
6
0 5 10 15 20 25 30 35 40

Fig. 7 Horizontal to vertical spectral ratio amplification for afternoon data on 280510.

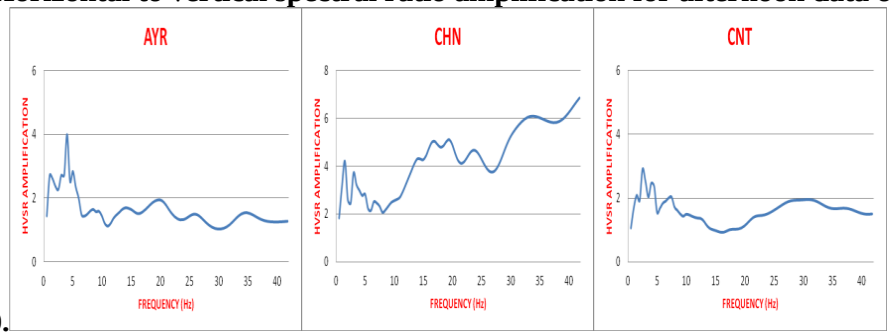

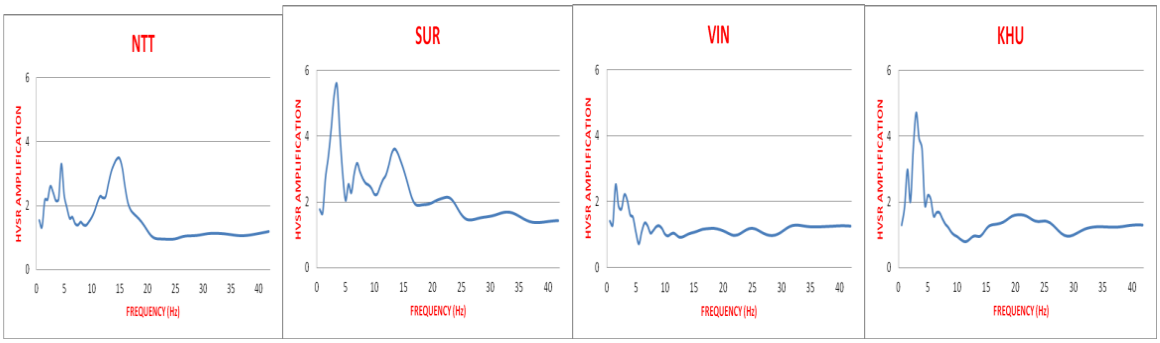

Fig. 8 Horizontal to vertical spectral ratio amplification for for morning data on 010510.

Table 3 Predominant frequencies and amplification factors at various sites from the analysis of four samples of microtremor data.

No.	Station Name	Station code	Predominant Frequency (Fo)				H/V Amplification factors			
			220610	280510	130510	10510	220610	280510	130510	10510
1	Ayarchali	AYR	3.5	2.0	3.4	4.4	5.3	2.0	3.5	3.3
2	Chandrabadni	CHN	23.6	36.4	31.2	34.4	7.4	3.3	6.2	6.1
3	Chintarbagi	CNT	3.3	2.8	3.9	2.8	2.7	2.4	3.0	2.7
4	Khurmola	KHU	3.5	3.8	3.5	3.4	5.2	3.9	6.1	4.6
5	New Tehri	NTT	2.0	2.1	3.4	14.4	2.1	2.6	2.9	3.5
6	Pratapnagar	PRT	2.1	3.3			2.9	2.9		
7	Srikot	SRT	2.9	4.8	22.6		2.3	2.7	2.1	
8	Surkanda Devi	SUR		2.9	4.2	3.6		5.0	4.5	4.8
9	Giyanja	GYN	2.2	2.1	2.8		5.1	3.8	4.4	
10	Rajgadi	RAJ	2.2	2.0	3.8		2.1	1.7	1.6	
11	Vinakkhal	VIN	3.3	3.4	12.3	2.0	1.8	2.1	1.8	1.8

Conclusions

The estimates of site effects ssing S–wave spectral ratio method shows higher amplification at sites located nearest to the epicenters of the earthquakes as compared to sites located away from the epicenters. Almost similar frequency dependent trend in the S-wave site amplification in the radial and transverse components has been brought out at majority of sites relative to PRT site. This type of response seems to be attributed to almost similar geological environments below the recording sites. The sites located closer to the Main Central Thrust (MCT) barring RAJ site such as GYN, KHU and

VIN have broad amplification peaks around 4 Hz to 5 Hz. High amplification at CHN site seems to be due to the high topography of the site.VIN, AYR sites are located at almost same distance from the source and have brought out almost similar trend in the site amplification in all the three components. At all the sites, the vertical component show consistently low site amplification as compared to horizontal components particularly at frequencies above 4 Hz to 5 Hz. By HVSR method, for the early morning record of microtremors, it has been observed that the response at CNT, PRT, NTT and RAJ site are almost similar with a broad peak around 4 Hz. The dominant peaks are between 3Hz to 4 Hz. At NTT and AYR sites a sharp peak embedded in a broad peak around 5 Hz has been brought out. The sharp peak around 4 Hz seems to be due to the continuous vibrations generated by the operation of turbines which are within the radius of 2 km to 3 km from the sites. Using HVSR method, for the afternoon record, it has been observed that at all the sites maximum peaks are in between 2 Hz to 4 Hz and the amplification values go on decreasing beyond 4 Hz. The amplification factors are found to be non-linear functions of the frequency.

References

1. Aki K. (1969). Analysis of seismic coda of local earthquakes as scattered waves, J. Geophys. Res., 74, 615-631.
2. Aki, K. and B. Chouet (1975). Origin of coda waves: source, attenuation, and scattering effects,J.Geophys. Res. 80, 3322-3342.
3. Babita Sharma, Dinesh Kumar and S.S. Teotia. Site Amplification Factors in Koyna region using Coda waves, Indian Geophys, Union (October 2008), Vol 12, No. 4, 149-156.
4. Bonilla, L. F., J. H. Steidl, G. T. Lindley, A. G. Tumarkin, and R. J. Archuleta (1997). Site amplification in the San Fernando Valley, California: variability of site-effect estimation using the S-wave, coda and H/V methods. Bull. Seism. Soc. Am., 87, 710-730.
5. Borcherdt, R. D. (1970). Effects of local geology on ground motion near San Francisco Bay, Bull Seism. Soc. Am. 60, 29-61.
6. Borcherdt. R. D. and J. F. Gibbs (1976). Effects of local geological conditions in the region on ground motions and intensities of the 1906 earthquakes, Bull Seism. Soc. Am. 66, 467-500.
7. Boominathan A., Evaluation of amplification Hazard for Chennai city. First disaster management congress, New Delhi, Nov. 29-30, 2006.
8. Chin, B. H. and K. Aki (1991). Simultaneous determination of source, path, and recording site effects on strong ground motion during the Loma Prieta earthquake: a preliminary result on pervasive nonlinear site effect, Bull. Seism. Soc. Am. 81, 1859-1884.
9. EQ: 2011-26 (2012). Report on Processing and interpretation of seismological data collected from January 2010to December 2010 employing seismological network around Tehri region, unpublished technical report of Department of Earthquake Engineering, Indian Institute of technology Roorkee, Roorkee.
10. Feng Su, John G. Anderson, James N. Brune. A comparison of Direct S –Wave and Coda Wave site amplification determined from aftershocks of the Little Skull Mountain Earthquake, Bull. Seism. Soc. Am. 86, 1006-1018.
11. Hartzell, S. H., A. Leeds, A. Frankel, and J. Michael (1996). Site response for urban Los Angeles using aftershocks of the Northridge earthquake, Bull. Seism. Soc. Am. 86, S168-S192.
12. Havskov J. & L. Ottemoller (2009). Processing of Earthquake data (Preliminary version) PP-101.
13. J- SESAME user manual Version 1.08 (2004). The J-SESAME software, the utility programs developed within the framework of the EU project SESAME (EVG1-CT-2000-00026) for "Site Effects Assessment Using Ambient Excitations."
14. Kumar D., I. Sarkar, Sri Ram, and K.N. Khattri (2005). Estimation of the source parameters of the Himalaya earthquake of October 19, 1991, average effective shear wave attenuation parameter and local site effects from accelerograms, Tectonophysics, 407, 1-24.
15. Kato, K., K. Aki, and M. Takemura (1995). Site amplification from coda waves: validation and application to S-wave site response. Bull. Seism. Soc. Am. 85, 467-477.
16. Koyanagi, S., K. Mayeda and K. Aki (1992). Frequency-dependent site amplification factors using the S-wave coda for the island of Hawaii, Bull. Seism. Soc. Am. 82, 1151-1185.

17. Lachet, D., C. Hatzfeld, P.Y. Bard, N. Theodulis, C. Papaioannou, and A. Savvaidis (1996). Site effects and microzonation in the city of Thessaloniki (Greece), comparison of different approaches, Bull. Seism. Soc. Am. 86, 1692-1703.
18. Margheriti L., L. Wennerberg, and J. Boatwright (1994). A comparison of coda and S-wave spectral ratio estimates of site response in the southern San Francisco Bay area, Bull. Seism. Soc. Am. 84, 1815-1830.
19. Mayeda, K., S. Koyanagi, and K. Aki (1991). Site amplifications from S wave coda in the Long Valley caldera region, California, Bull. Seism. Soc. Am. 81, 2194-2213.
20. Nakamura Y. (1989). A method for dynamic characteristics estimation of subsurface using microtremors on the ground surface. *Q. Rep. RTRI3Q* (1989), pp. 25-33.
21. Nath S.K., P. Sengupta, S.Sengupta, and A. Chakarberti (2000). Site response estimation using strong motion network:A step towards microzonation of the Sikkim Himalayas, Current Science, 79, 1316-1326.
22. Nath S.K., Sengupta P., Srivastav S.K., Bhattacharya S.N.,Dattatrayam R.S., Prakash R. & Gupta H.K. (2003). Estimation of S-wave site response in and around Delhi region from weak motion data, Earth, Planet Sc., 112, 441-462.
23. Phillips, W. S. and K. Aki (1986). Site amplification of coda waves from local earthquakes in central California. Bull. Seism. Soc. Am. 76, 627- 648.
24. Raution, T. G. and V. I. Khalturin (1978). The use of Coda for determination of earthquake spectrum, Bull. Seism. Soc. Am. 68, 923-948.
25. Reipl, J., Bard, P. Y., Hartzfeld, D., Papaioannou, C. and Nechtschein, S. (1998). Detailed evaluation of site response estimation methods across and along the sedimentary valley of Volvi (EURO- SEISTEST), Bull. Seism. Soc. Am. 88 (2), 488-502.
26. Rekhi G. (2010). Site amplification characteristics of Garhwal Lesser Himalaya Using S-wave and Coda waves, M. Tech. Dissertation, DEQ, IIT Roorkee, 42 pp.
27. Sharma B., D. Kumar and S.S.Teotia (2008). Site Amplification Factors in Koyna Region using Coda Waves, J. Ind. Geophys, Union Vol.12, No.4, 149-156.
28. Su, F. and K. Aki (1995). Site amplification factors in central and southern California determined from coda waves, Bull. Seism. Soc. Am. 85, 452-466.
29. Steidl, J. H., A. G. Tumarkin, and R. J. Archuleta (1996). What is a reference site? Bull. Seism. Soc. Am. 86, 1733-1748.
30. Tsujiuara, M. (1978). Spectral analysis of the coda waves from local earthquakes, Bull. Earthqauke Res. Inst. Tokyo Univ. 53, 1-48.